Article

Comparison of Two Processes Forming CaCO$_3$ Precipitates by Electrolysis

Hyun Sic Park [1], JunYoung Han [2], Ju Sung Lee [1], Kwang-Mo Kim [3], Hyung Jun Jo [1] and Byoung Ryul Min [1,*]

[1] Department of Chemical and Biomolecular Engineering, Yonsei University, 262 Seongsanno, Seodaemun-gu, Seoul 120-749, Korea; ethic-life@hanmail.net (H.S.P.); smilelee2@naver.com (J.S.L.); mirage0515@naver.com (H.J.J.)

[2] Department of Chemistry and Chemical Biology, Rensselaer Polytechnic Institute, Troy, NY 12180, USA; jy1204@gmail.com

[3] COSMAX #603, Pangyo Inno Valley, 255, Pangyo-ro, Bundang-gu, Seongnam-si, Gyeonggi-do 13486, Korea; a_rod1985@hotmail.com

* Correspondence: minbr345@yonsei.ac.kr; Tel.: +82-2-2123-2757

Abstract: As one of the carbon capture and utilization (CCU) technologies, mineral carbonation which has been introduced to reduce the carbon dioxide (CO$_2$) concentration in the atmosphere is a technology that makes it possible to capture CO$_2$ and recycle byproducts as resources. However, existing mineral carbonation requires additional energy and costs, as it entails high temperature and high pressure reaction conditions. This study compared two processes which electrolyze NaCl and CaCl$_2$ solution to produce CO$_2$ absorbent needed to generate CaCO$_3$, and which were conducted at room temperature and pressure unlike existing mineral carbonation. As a result, high-purity calcite was obtained through Process 1 using NaCl solution, and aragonite and portlandite were obtained in addition to calcite through Process 2 (two steps) using CaCl$_2$ solution.

Keywords: mineral carbonation; CaCO$_3$; electrolysis

1. Introduction

Carbon dioxide (CO$_2$) accounts for more than 88% of greenhouse gas emissions and has contributed more than 55% to the greenhouse effect [1,2]. In order to solve the climate change and environmental problems caused by CO$_2$, a number of studies have been carried out actively [1,3,4].

Until now, intensive research has been conducted on carbon capture and storage (CCS) technologies to store the CO$_2$ underground or on the seabed and carbon capture and utilization (CCU) technologies to capture CO$_2$ and convert it to be reused. However, it has become known that there are several problems in the practical application of these techniques [5]. In the case of CCS, excessive energy consumption throughout the entire process and the possibility of leakage of absorbent have been pointed out as the biggest problems [6]. CCU technology was introduced as a partial alternative to these problems. Among the CCU technologies, mineral carbonation is one of the most discussed techniques for treating large amounts of CO$_2$. However, the magnesium-based mineral carbonation process is also complicated and should be conducted in high temperature and high pressure conditions, so the facility where it is conducted needs to be equipped for the high risk group [7–9]. For this reason, this study introduces a mineral carbonation process undertaken with less energy by using electrolysis technology with a porous ceramic membrane as ion channel and separator. In this process, divalent metal cations are combined with CO$_2$ to form carbonate minerals [10]. Generally, CO$_2$ reacts with the alkaline absorbent solutions. In the existing carbonation process, magnesium hydroxide was

primarily used to produce the alkaline solution, because the Mg-containing minerals contain about 40% Mg^{2+}, while the Ca-containing minerals contain about 10%–15% Ca^{2+} [11]. However, the existing magnesium-based carbonation process has the aforementioned problems. According to Nduagu [12] and Khoo et al. [13], extracting magnesium oxide or hydroxide from serpentine requires heating to a temperature of 500 °C or higher, and high temperature reaction conditions are needed again in the hydration process after extraction [14].

To reduce these problems, our previous study and this study have introduced a process of electrolyzing chloride salts present in seawater and producing alkaline solution, which is a CO_2 absorbent. Our process does not extract oxides and hydroxides from rocks, but uses electrolysis at room pressure and room temperature to obtain hydroxides. More specifically, in our previous report [15], a calcium carbonation process using NaCl solution was introduced. The entire process is divided into three steps: electrolysis of NaCl (sodium hydroxide formation), reaction with CO_2 (sodium bicarbonate formation), and carbonation (generation of calcium carbonate). Through this process, we were able to obtain $CaCO_3$ in the form of calcite in a stable manner. However, since NaCl solution is used for NaCl process, Ca^{2+} should be added to the carbonation process in order to replace Na^+. In addition, the process of precipitating the carbonate after this substitution process is complex and requires considerable time.

Therefore, in this study, in order to simplify process and increase energy efficiency, $CaCl_2$ in seawater was used to make alkaline solution, so that the process of Ca^{2+} addition was eliminated and the process was reduced to two steps, unlike in our previous study. Since the substitution process is not required, the carbonation process is simpler than the NaCl solution process. Additionally, it was expected that more products could be obtained because of the high content of calcium ions contained in the carbonation process. Precipitates would also be formed more quickly through this process, and the consumption of energy would be decreased. This present work focuses on the comparison of the characterization and yield of final products for our previous and proposed processes.

2. Materials and Methods

2.1. Materials

NaCl (99.5%) and $CaCl_2$ (95.9%) were purchased from Samchun Chemical Korea and Kanto Co., Tokyo, Japan, respectively, and used as received. Pure CO_2 (99.0%) gas was purchased from Samheung, Gyeonggi-do, Korea, and was used without any pretreatment. Pure $CaCO_3$ ($\geq$99.0%, Sigma-Aldrich, St. Louis, MO, USA) was used to compare with the final $CaCO_3$ product from the two processes. Ultra-pure water prepared from AquaMax 311 (YL Instrument Co. Ltd, Anyang, Korea) was used in all processes.

2.2. Electrolysis Device

The electrolysis device is shown in Figure 1. Each of the units is the same as those used before [15]. The anode (carbon) is located in the center of a round ceramic membrane. The electrodes of the cathode (stainless) were installed at the same distance around the anode. The mean pore size of the porous ceramic membrane was 0.2 μm, which acts as an ion channel when the electrolytic process is started. In other words, ion separation occurs between the inner and outer reactor during the electrolysis process. After the electrolytic process, fine CO_2 bubbles (100–400 μm) were injected from the generator (ANGEL AQUA, Changwon, Korea). At this time, this ceramic wall plays as an ion separator.
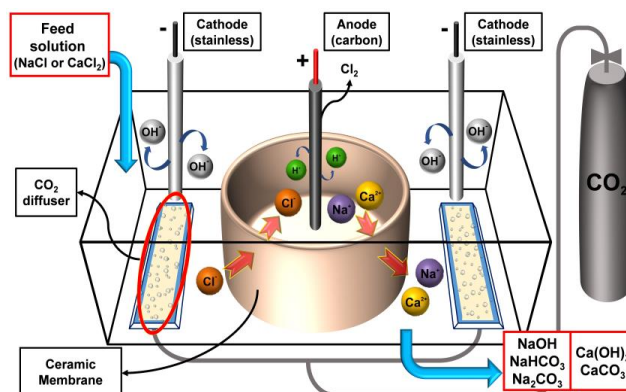
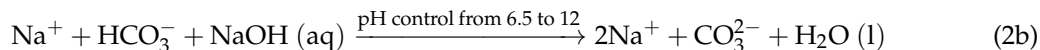**Figure 1.** Schematic diagram of the electrolysis device.

2.3. NaCl Solution Process: Process 1

In the case of the NaCl solution process (Process 1), the experiment to generate $CaCO_3$ was carried out in three steps, preparing 2%–6% NaCl solution based on the concentration of coastal seawater and deep seawater. Depending on 1–4 A of current intensity, electrolysis of NaCl solution was required to react for 10–15 min at 25 °C and 1 bar, and voltage was about 8–24 V. Characterization of the product was reported in our earlier paper [15], and chemical reaction of each step was summarized as follows:
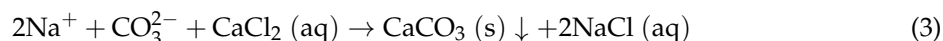
Step 1:

$$2NaCl\,(aq) + 2H_2O \xrightarrow{\text{electrolysis}} 2Na^+ + 2OH^- + H_2\,(g) \uparrow + Cl_2\,(g) \uparrow \tag{1}$$

Step 2:

$$Na^+ + OH^- + CO_2\,(g) \rightarrow Na^+ + HCO_3^- \tag{2a}$$

$$Na^+ + HCO_3^- + NaOH\,(aq) \xrightarrow{\text{pH control from 6.5 to 12}} 2Na^+ + CO_3^{2-} + H_2O\,(l) \tag{2b}$$

Step 3:

$$2Na^+ + CO_3^{2-} + CaCl_2\,(aq) \rightarrow CaCO_3\,(s) \downarrow + 2NaCl\,(aq) \tag{3}$$
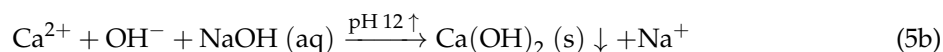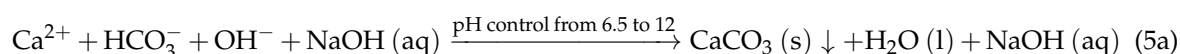
2.4. CaCl₂ Solution Process: Process 2

In the case of the CaCl₂ solution process (Process 2), the experiment to generate $CaCO_3$ was performed in two steps, as 0.5%–2% CaCl₂ is based on the concentration of seawater. All other parameters are the same as in Process 1. The reaction time was stopped at the point where there is almost no variation in pH, at around 11.6. Under the same conditions, the reaction time of electrolysis in Process 2 took 5 min less than in Process 1.

In Step 1, an alkaline calcium hydroxide solution used as an absorbent of CO_2 was produced through electrolysis, and the reaction is as follows:

$$CaCl_2\,(aq) + 2H_2O\,(l) \xrightarrow{\text{electrolysis}} Ca^{2+} + 2OH^- + H_2(g) \uparrow + 2Cl_2(g) \uparrow \tag{4}$$

In Step 2, calcium hydroxide solution was formed by a ceramic membrane at the negative electrode side after electrolysis. $CaCO_3$ was precipitated by blowing CO_2 at constant flow rate (2 L·min^{-1}). The precipitation reaction is as follows:

$$Ca^{2+} + HCO_3^- + OH^- + NaOH\,(aq) \xrightarrow{\text{pH control from 6.5 to 12}} CaCO_3\,(s) \downarrow + H_2O\,(l) + NaOH\,(aq) \tag{5a}$$

$$Ca^{2+} + OH^- + NaOH\,(aq) \xrightarrow{\text{pH 12} \uparrow} Ca(OH)_2\,(s) \downarrow + Na^+ \tag{5b}$$

A side reaction as in Equation (5b) occurs when the pH value is higher than 12.

2.5. Characteristics of Precipitates

The final product $CaCO_3$ was obtained by GF/C film (Whatman® Glass microfiber filters, Whatman, Clifton, NJ, USA) filtration and drying for 24 h at 80 °C. Fourier transform infrared (FT-IR) spectra were obtained with a Spectrum 100 FT-IR Spectrometer, PerkinElmer connected attenuated total reflection (ATR) tool (PerkinElmer, Norwalk, CT, USA). X-ray diffraction (XRD) was measured using a Rigaku Ultima IV (XRD, Ultima IV, RIGAKU, Tokyo, Japan) using a Cu Kα X-ray 40 kV/30 mA, and the range was 2θ = 15°–70°. The shape and particle size of the fully dried samples were investigated by field emission scanning electron microscopy (FE-SEM, JEOL-7800F, Tokyo, Japan).

3. Results

3.1. Fourier Transform Infrared Analysis

Figure 2 shows the IR spectra measured in the 1800–600 cm^{-1} range of the respective samples. All $CaCO_3$ products from Process 1 and Process 2 were confirmed as calcite, and the peaks were 1418, 876, and 713 cm^{-1}. Interestingly, the IR spectrum of $CaCO_3$ obtained from Process 2 was observed for new peaks. The value of the peak observed in the 1500–1400 cm^{-1} region and the 700–650 cm^{-1} region is the peak of $CaCO_3$ as aragonite (respectively, 1465 cm^{-1}, C–O, stretching mode; 692 cm^{-1}, C–O, out-plane bending), and the peak in the 850–800 cm^{-1} region is the value of the peak only as vaterite and aragonite (848 cm^{-1}, C–O, in-plane bending) [16,17]. In addition, the peak (1080 cm^{-1}) in the 1100–1000 cm^{-1} region is the stretching mode of the O–C–O functional group.
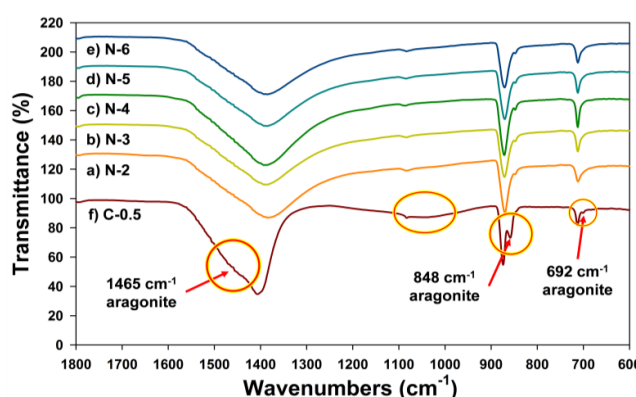

Figure 2. Fourier transform infrared (FT-IR) spectrum of the precipitated particles through Process 1 and Process 2. (**a**) N-2; (**b**) N-3; (**c**) N-4; (**d**) N-5; (**e**) N-6; and (**f**) C-0.5 (range of 1800–600 cm^{-1}). Product particles formed using $CaCl_2$ 0.5% solution are termed as C-0.5, while product particles formed using NaCl are termed as N-X, where X is the NaCl concentration.

3.2. X-ray Diffraction Analysis

XRD patterns were analyzed for more accurate compositional analysis of the generated particles and the results are shown in Figure 3. The product of Process 1 is that characteristic peaks of calcite only appear through our previous studies. In XRD pattern analysis of the products of Process 2, it was possible to confirm the two-theta values for aragonite (26.3, 27.2) and for $Ca(OH)_2$ (34.1, 47.1), as well as the two-theta value for calcite (29.3, 39.3, 43.1) [18].

According to the research of Ma et al. [19], crystalline forms of $CaCO_3$ are greatly influenced by the pH of the water soluble matrix (WSM), and it has been reported that aragonite crystal forms can be obtained at low pH levels (pH 5.5–9.0). For Process 2, after forming a $Ca(HCO_3)_2$, $CaCO_3$ was precipitated by adjusting the pH in the last step. Thus, as reported in the case where the precipitation starts from a low pH level, aragonite crystals can be obtained. However, as the pH level gradually increases, it is determined that crystalline calcite was also generated, as well as

aragonite [20]. Furthermore, the $Ca(OH)^-$ which exists in the form of hydroxide ions is converted into $Ca(OH)_2$ and precipitates by pH control [21]. For Process 1, after adjusting the pH to 12 or higher by using NaOH solution, precipitation was started through substitution reaction with the calcium ions. Thus, if the precipitation is started at a high pH, it is possible to obtain only the hexahedral form of calcite precipitation [20,22].
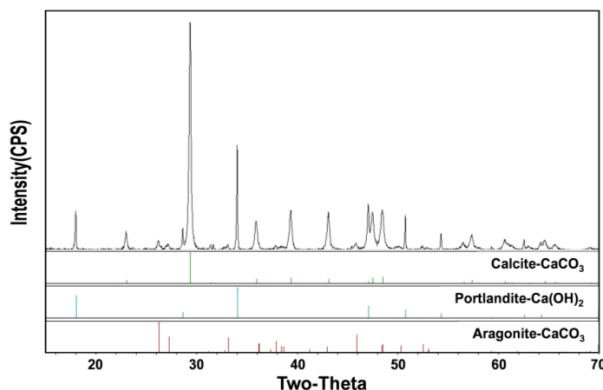

Figure 3. The X-ray diffraction (XRD) spectra of the produced particles from Process 2.

3.3. Field Emission Scanning Electron Microscopy Image Analysis

FE-SEM was used to confirm other characteristics of other formed particles. Figure 4 is the SEM image of formed particles pictured at ×10,000 magnification. From Figure 4, numerous differences were observed in the size and shape of formed particles. The size of formed particles obtained from Process 1 is 3–4 μm, regardless of the concentration of feed solution, and the particles formed were cubic calcite. On the other hand, formed particles obtained from Process 2 were smaller than 1 μm, and it was observed that several shapes of particles exist. When the $CaCO_3$ crystals are formed at high pH, crystal nucleation proceeds rapidly and affects particle size [19].
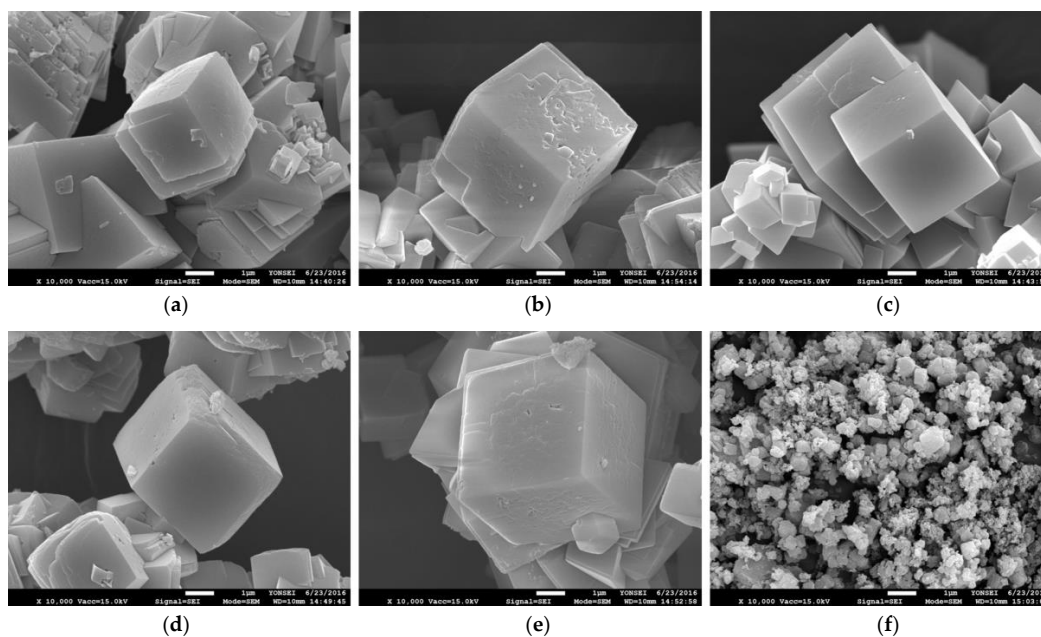

Figure 4. Scanning electron microscopy (SEM) image of the precipitated particles through Process 1 and Process 2 (×10,000 magnification). (**a**) N-2; (**b**) N-3; (**c**) N-4; (**d**) N-5; (**e**) N-6; and (**f**) C-0.5.

According to the research of Westin and Rasmuson [23], the growth rate of calcite was 4.29×10^{-6} mol·m^{-2}·s^{-1} and that of aragonite was 1.31×10^{-6} mol·m^{-2}·s^{-1} under the same reaction conditions. In the case of Process 2, the intensity of calcite peak was strong, as shown in IR and XRD spectra. It was assumed that numerous calcites whose growth rates were faster in three times were formed. Additionally, in the case of Process 2, in which a crystalline product is formed with an additional product through a side reaction, it is confirmed that the size of the particles is smaller compared to the products of Process 1, due to a hindrance of growth between particles.

3.4. Conversion Yield of Precipitate

Figure 5 shows the average conversion rate of formed precipitates in two processes. The rates for the two processes were calculated by the rate of theoretical value and measured value for overall Ca^{2+} contained in used solution in the final step, which is the precipitation procedure. In Process 1, conversion rate increased as the concentration of feed solution increased. However, it was confirmed that the average conversion rate was 77.7% in 5% solution, and it was decreased in 6% solution. In Process 2, the average conversion rate of precipitates was 90.0% in 0.5% solution, which is more than 10% higher than the highest value shown in Process 1. The reason for this difference is that Na^+ and Ca^{2+} of the formed absorbents reacted with different amount of CO_3^{2-}, although the overall amount of supplied CO_2 gas was the same in all experiments. In addition, the reason that conversion rate was decreased in high concentration $CaCl_2$ solution was because precipitates were not dramatically increased compared to the increased amount of Ca^{2+}.
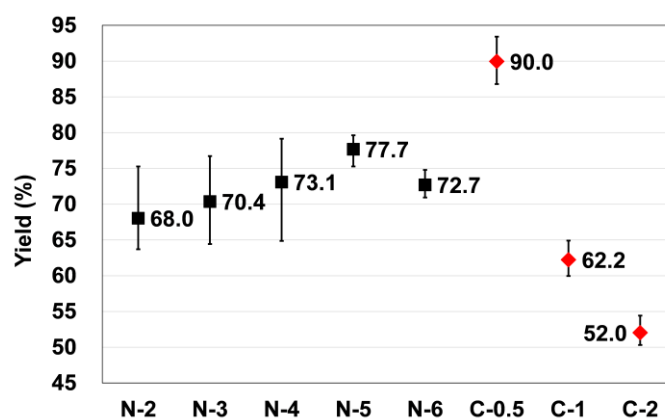

Figure 5. Conversion rate of precipitates for each concentration feed solution used in Process 1 and Process 2.

4. Conclusions

In this study, attempts to minimize the problems of existing CCS techniques were made by using Na^+ and Ca^{2+} contained in sea water, and two processes for capturing CO_2 and producing carbonate were compared and analyzed. The process of the two methods that we have presented can be compared in three major ways.

First, it is possible to be approached from the energy perspective. Both processes form precipitates in a thermodynamically stable form. Additionally, the overall process uses reaction conditions of room temperature and pressure. This demonstrates that $CaCO_3$ can be produced quickly and stably using less energy than conventional methods requiring high-temperature and high-pressure reaction conditions, which was proven through structural analysis using FT-IR spectra. Further, the energy consumption of Process 2 was small compared to Process 1, through simplification to a two-step process and reduced process time of electrolysis reaction. In addition, the carbonation process is an exothermic reaction, and does not require additional energy [24].

Second, it is possible to be approached by added value of formed precipitates. The result of SEM imaging and XRD pattern analysis of the precipitate produced showed that $CaCO_3$ produced by Process 1 could be used as chemical material without any purification process after it was produced with high purity calcite. This has also been proven through our previous studies. On the other hand, in the precipitate produced by Process 2, aragonite—another crystal form of $CaCO_3$—was identified along with portlandite. Aragonite precipitate is a raw material used widely, not only in plastic, rubber, paint, and paper, but also in feeds and pharmaceuticals. If only aragonite $CaCO_3$ is to be formed, 50–70 °C temperature should be used as reaction conditions [25]. It is also possible to weakly control the size of precipitates by controlling pH. Through this process, purity and shape control of aragonite can be applied as raw material in various fields.

Finally, it is possible to be approached from the perspective of CO_2 reduction, as it relates to global warming. In this perspective, it was assumed that Process 2, for which the reaction conversion rate was 10% higher than Process 1, captured more CO_2. Furthermore, the final product of Process 2 can process more CO_2 than that of Process 1, and can be used as raw material for construction materials [26].

Thus, using Process 2 makes it possible to obtain a precipitate with a high added value more quickly and easily than Process 1. In addition, this study was processed as batch reaction. If precipitates are produced by continuous reactor, solutions left after reaction can be used again in the reaction by reprocessing. Therefore, it is possible to minimize environmental problems caused by waste liquor formed in the process. In addition, natural $CaCO_3$ formation generally requires long reaction time, as stated in the previous study [15]. On the contrary, both processes we have proposed can reduce the reaction time to form $CaCO_3$.

As mentioned earlier, conventional mineral carbonation is subject to the process of extracting the reaction components. According to Kakizawa et al. [27], it consumes 1.27 MW of energy in the process for extracting calcium ion from calcium silicate. However, in our studies, extraction process was excluded. In actual seawater application, a membrane enrichment system would be used, which would feed the reaction components through separation and concentration by the membrane.

More research is needed, but we hope to contribute to the reduction of atmospheric CO_2 through carbonation of CO_2 based on these considerations.

Author Contributions: Hyun Sic Park, JunYoung Han and Byoung Ryul Min conceived and designed the experiments; Hyun Sic Park performed the experiments; Hyun Sic Park and JunYoung Han analyzed the data; Ju Sung Lee, Kwang-Mo Kim and Hyung Jun Jo contributed reagents/materials/analysis tools; Hyun Sic Park wrote first draft; Byoung Ryul Min revised the paper.

Conflicts of Interest: The authors declare no conflict of interest.

References

1. Yu, K.M.K.; Curcic, I.; Gabriel, J.; Tsang, S.C.E. Recent advances in CO_2 capture and utilization. *ChemSusChem* **2008**, *1*, 893–899. [CrossRef] [PubMed]

2. West, T.O.; Pena, N. Determining thresholds for mandatory reporting of greenhouse gas emissions. *Environ. Sci. Technol.* **2003**, *37*, 1057–1060. [CrossRef] [PubMed]

3. Baciocchi, R.; Corti, A.; Costa, G.; Lombardi, L.; Zingaretti, D. Storage of carbon dioxide captured in a pilot-scale biogas upgrading plant by accelerated carbonation of industrial residues. *Energy Procedia* **2011**, *4*, 4985–4992. [CrossRef]

4. Holloway, S. Underground sequestration of carbon dioxide a viable greenhouse gas mitigation option. *Energy* **2005**, *30*, 2318–2333. [CrossRef]

5. Siefert, N.S.; Litster, S. Exergy and economic analyses of advanced IGCC-CCS and IGFC-CCS power plants. *Appl. Energy* **2013**, *107*, 315–328. [CrossRef]

6. Damen, K.; Faaij, A.; Turkenburg, W. Health, safety and environmental risks of underground CO_2 storage–overview of mechanisms and current knowledge. *Clim. Chang.* **2006**, *74*, 289–318. [CrossRef]

7. Lackner, K.S.; Butt, D.P.; Wendt, C.H. Progress on binding CO_2 in mineral substrates. *Energy Convers. Manag.* **1997**, *38*, S259–S264. [CrossRef]

8. Fagerlund, J.; Nduagu, E.; Zevenhoven, R. Recent developments in the carbonation of serpentinite derived $Mg(OH)_2$ using a pressurized fluidized bed. *Energy Procedia* **2011**, *4*, 4993–5000. [CrossRef]

9. Fagerlund, J.; Nduagu, E.; Romao, I.; Zevenhoven, R. CO_2 fixation using magnesium silicate minerals part 1: Process description and performance. *Energy* **2012**, *41*, 184–191. [CrossRef]

10. Oelkers, E.H.; Gislason, S.R.; Matter, J. Mineral carbonation of CO_2. *Elements* **2008**, *4*, 333–337. [CrossRef]

11. Goff, F.; Lackner, K. Carbon dioxide sequestering using ultramafic rocks. *Environ. Geosci.* **1998**, *5*, 89–101. [CrossRef]

12. Nduagu, E. Mineral Carbonation: Preparation of Magnesium Hydroxide [$Mg(OH)_2$] from Serpentinite Rock. Master's (Eng) Thesis, Åbo Akademi University, Åbo, Finland, 2008.

13. Khoo, H.; Bu, J.; Wong, R.; Kuan, S.; Sharratt, P. Carbon capture and utilization: Preliminary life cycle CO_2, energy, and cost results of potential mineral carbonation. *Energy Procedia* **2011**, *4*, 2494–2501. [CrossRef]

14. Stasiulaitiene, I.; Fagerlund, J.; Nduagu, E.; Denafas, G.; Zevenhoven, R. Carbonation of serpentinite rock from Lithuania and Finland. *Energy Procedia* **2011**, *4*, 2963–2970. [CrossRef]

15. Park, H.S.; Lee, J.S.; Han, J.; Park, S.; Park, J.; Min, B.R. CO_2 fixation by membrane separated NaCl electrolysis. *Energies* **2015**, *8*, 8704–8715. [CrossRef]

16. Tlili, M.; Amor, M.B.; Gabrielli, C.; Joiret, S.; Maurin, G.; Rousseau, P. Characterization of caco$_3$ hydrates by micro-raman spectroscopy. *J. Raman Spectrosc.* **2002**, *33*, 10–16. [CrossRef]

17. Wu, G.; Wang, Y.; Zhu, S.; Wang, J. Preparation of ultrafine calcium carbonate particles with micropore dispersion method. *Powder Technol.* **2007**, *172*, 82–88. [CrossRef]

18. McMurdie, H.F.; Morris, M.C.; Evans, E.H.; Paretzkin, B.; Wong-Ng, W.; Ettlinger, L.; Hubbard, C.R. Standard X-ray diffraction powder patterns from the jcpds research associateship. *Powder Diffr.* **1986**, *1*, 64–77. [CrossRef]

19. Ma, Y.; Gao, Y.; Feng, Q. Effects of pH and temperature on $CaCO_3$ crystallization in aqueous solution with water soluble matrix of pearls. *J. Cryst. Growth* **2010**, *312*, 3165–3170. [CrossRef]

20. Stocks-Fischer, S.; Galinat, J.K.; Bang, S.S. Microbiological precipitation of $CaCO_3$. *Soil Biol. Biochem.* **1999**, *31*, 1563–1571. [CrossRef]

21. Ren, L.; Zhang, Y.; Bian, Y.; Liu, X.; Liu, C. Investigation of quartz flotation from decarburized vanadium-bearing coal. *Physicochem. Probl. Miner. Process.* **2015**, *51*, 755–767.

22. Han, Y.S.; Hadiko, G.; Fuji, M.; Takahashi, M. Crystallization and transformation of vaterite at controlled pH. *J. Cryst. Growth* **2006**, *289*, 269–274.

23. Westin, K.-J.; Rasmuson, A.C. Crystal growth of aragonite and calcite in presence of citric acid, DTPA, EDTA and pyromellitic acid. *J. Colloid Interface Sci.* **2005**, *282*, 359–369. [CrossRef] [PubMed]

24. Wang, X.; Maroto-Valer, M.M. Integration of CO_2 capture and mineral carbonation by using recyclable ammonium salts. *ChemSusChem* **2011**, *4*, 1291–1300. [CrossRef] [PubMed]

25. Colfen, H.; Qi, L. A systematic examination of the morphogenesis of calcium carbonate in the presence of a double-hydrophilic block copolymer. *Chemistry* **2001**, *7*, 106–116. [CrossRef]

26. Iizuka, A.; Fujii, M.; Yamasaki, A.; Yanagisawa, Y. Development of a new CO_2 sequestration process utilizing the carbonation of waste cement. *Ind. Eng. Chem. Res.* **2004**, *43*, 7880–7887. [CrossRef]

27. Kakizawa, M.; Yamasaki, A.; Yanagisawa, Y. A new CO_2 disposal process via artificial weathering of calcium silicate accelerated by acetic acid. *Energy* **2001**, *26*, 341–354. [CrossRef]